Kinetic Energy of Liquid and Solid ^{4}He

D. M. Ceperley,[1,2] R. O. Simmons,[2,3] and R. C. Blasdell[2,3]
[1]*National Center for Supercomputing Applications, University of Illinois at Urbana-Champaign, 1110 W. Green Street, Urbana, Illinois 61801*
[2]*Department of Physics, University of Illinois at Urbana-Champaign, 1110 W. Green Street, Urbana, Illinois 61801*
[3]*Frederick Seitz Materials Research Laboratory, University of Illinois at Urbana-Champaign, 1110 W. Green Street, Urbana, Illinois 61801*
(Received 1 April 1996)

We report new path-integral calculations and measurements of the kinetic energy of condensed helium and construct an overall dependence of kinetic energy on temperature for densities less than 70 atoms nm^{-3}. In the solid phase we find the kinetic energy is almost temperature independent and, surprisingly, has a smaller kinetic energy than the fluid near freezing at the same density. In the high temperature fluid phase, the excess kinetic energy decreases to zero very slowly because of pair scattering from the repulsive interatomic potential. [S0031-9007(96)00592-3]

PACS numbers: 64.70.Dv, 61.12.Ex, 67.20.+k, 67.80.Gb

The momentum distributions of the condensed isotopes of helium have been a matter of widespread interest for many years because of their connections with the theories of Bose condensation and of Fermi liquids. In this Letter we consider only the second moment of the momentum distribution, the kinetic energy E_k. In contrast to the potential energy, the kinetic energy of a many-body system has distinctly different properties in the classical regime (Maxwellian), the quantum liquid, the crystal (Debye-like), the superfluid (Bose condensation), and for liquid ^{3}He (Fermi-liquid behavior). Helium is a nearly ideal system in which to study the variation of these quantum effects because of the wide range of densities, temperatures, and phases that can be achieved experimentally and retained stably in the laboratory (unlike, for example, nuclear matter or laser-cooled ions). The kinetic energy is difficult to measure directly; inelastic (quasielastic) neutron scattering at high momentum transfers is probably the best way. On the theory side, the interatomic potential of helium is better known [1] than for any other atomic and molecular system, and for bosonic ^{4}He one has a well-developed and highly accurate simulation method, path integral Monte Carlo (PIMC) [2]. Hence, ^{4}He is the simplest quantum system for which to make accurate comparisons of theory and experiment.

Here we make a critical comparison between various experiments and the PIMC theory and draw conclusions about the behavior of the kinetic energy upon melting and at higher temperatures. We first recapitulate our experimental and theoretical methods, and show that the results are in agreement. We then summarize our comprehensive picture of the kinetic energy of ^{4}He and comment on recent experiments.

With the advent of intense pulsed neutron sources, direct measurement of single-particle momentum distributions is possible within the limit of the impulse approximation [3]. Then the dynamic structure factor $S(\mathbf{Q}, E)$ for a target of mass m can be scaled to the longitudinal neutron Compton profile $J(y, \mathbf{Q})$ using the variable $\mathbf{y} = (m/h^2Q)(E - \hbar^2Q^2/2m)\hat{\mathbf{O}}$, where $\hat{\mathbf{O}}$ is a unit vector in the direction of the wave-vector transfer $\mathbf{Q}$. Within this limit, $S(\mathbf{Q}, E)$ is proportional to the longitudinal momentum distribution $n(\mathbf{p})$. An early search [4] for a change in kinetic energy upon melting in ^{4}He used a comparison of pulsed neutron scattering from a liquid and solid sample at the same density so that the systematic effects of multiple scattering and final state effects (FSE) would largely cancel. Within the precision of these data (a few percent), no difference was found between the fixed-angle recoil scattering profiles of hcp and liquid ^{4}He at a density of 29 nm^{-3}.

Measurements in solid and normal liquid ^{4}He were considerably refined in a second generation of experiments using chopper spectrometers [5]. Special care was taken in the Monte Carlo simulation of the spectrometer-sample system [6]. Further, because the measurements were made at finite Q (mostly around 237 nm^{-1}), the magnitudes of the FSE were measured and quantitatively compared with calculations over a range of sample densities. In particular, the leading asymmetric correction to the scaled profile $J(y)$ [7] was computed using the pair potential and the PIMC-determined two-particle distribution function $g(r)$. A typical measured profile $J(y)$, shown in Fig. 1, allows a clean statistical analysis. The well-defined character of the wings of the profile can be contrasted, for example, to the results shown in Fig. 1 of Ref. [8].

During the past decade, the PIMC method has been developed to calculate a variety of thermodynamic properties of liquid and solid helium from first principles. This method allows calculations to be carried out using realistic interatomic potentials at precisely the density and temperatures of relevance without uncontrolled approximations. The new calculations reported here use a semiempirical potential [1]. We are able to do more precise calculations of the kinetic energy because we used an accurate

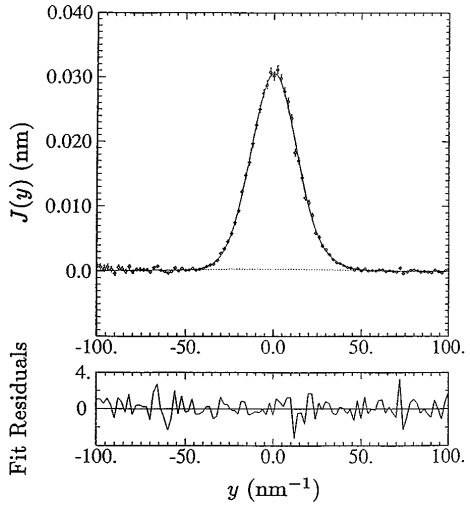

FIG. 1. Typical data of present pulsed neutron scattering experiment for liquid ^{4}He at 32.74 ± 0.23 nm^{-3} and 4.20 ± 0.04 K. Shown is a fit of a Gaussian momentum distribution $n(y)$ with Ref. [7] FSE corrections (solid line) to a measured neutron Compton profile $J(y)$ corrected for multiple scattering (circles). An effective instrumental resolution function determined by Monte Carlo simulation is convolved with the model $J(y)$. The fit residuals are shown at the bottom. For the fit, $\chi^2 = 87$ with 75 degrees of freedom.

pair density matrix to increase the time step to the value of 0.00625 K^{-1} at the higher densities and because we used the virial estimator [2] for energy instead of the thermodynamic estimator used previously. At a given temperature and density, the initial configurations of the paths were selected so as to match the proper experimental phase. Determination of the correct phase with PIMC would have been more difficult and possibly influenced by the neglected and ill-understood three-body potentials. In this Letter we neglect the effect of vacancies (or other defects) in the solid phase near melting. These could possibly raise the kinetic energy by $\approx$1 K at melting. Between 100 and 200 atoms were used in the present calculations. At the temperatures of concern in this Letter, we did not need to consider the effect of Bose statistics; that has been done in earlier calculations of the superfluid [2].

As a test, we have calculated the change in internal energy upon freezing and compared it with the value obtained from the experimental melting curve [9] and the Clausius-Clapeyron equation temperatures of 8.9 and 32 K. They differ by -0.3 K/atom at the lower temperature and 0.5 K/atom at the higher temperature, which is close to the combined statistical, systematic, and experimental errors for this quantity. Hence, by explicit tests we have established that the errors in the kinetic energy arising from the interatomic potential, the finite number of atoms, the time step, Bose statistics, and Monte Carlo sampling are less than 0.1 K/atom.

We have calculated the kinetic energy at about fifty different physical states and fit the energies in each phase. We included in the fitted data the zero temperature calculations [10,11]. In the solid phases we fit the kinetic energy by a form $E_k = a\rho^{\gamma_1} + (T/\rho^{\gamma_2}\Theta)^4$ with $\gamma_1 = 1.83$ and $\gamma_2 = 2.2$ while in the liquid phase we used a polynomial of the form $E_k = (3/2)T + \sum_{i,j} c_{i,j}\rho^i t^j$, where $t = [1 + (T/T_0)]^\eta$ and $T_0 \approx 3$ K and $\eta \approx -0.1$. Fitting errors are less than 0.2 K. We will publish the PIMC energies and fits elsewhere.

Figure 2 is a contour plot of the kinetic energy of liquid and solid ^{4}He. The superfluid phase (sf) and the liquid-gas region (l-g) are in the lower left-hand corner. (Note that the kinetic energy in the superfluid phase is given in Refs. [2,12,13]. In this Letter we do not address those regions of the phase diagram, concentrating instead on higher temperatures or densities.) First we discuss the kinetic energy in the solid, then at melting, and finally in the liquid. We remark that a purely classical system would have vertical, equally spaced contours, a behavior completely different from helium, at any density or temperature.

In the solid phase the kinetic energy depends almost entirely on density with only a small dependence on temperature, near melting, and only a small dependence

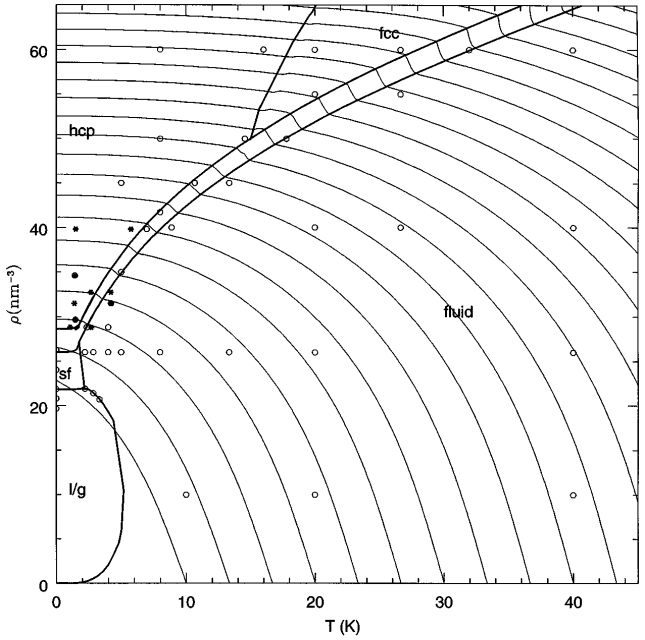

FIG. 2. Contour plot of the PIMC kinetic energy of ^{4}He as a function of temperature and density. The experimental phase transitions (to fluid, superfluid, hcp, and fcc crystals) are shown as dark lines. The kinetic energy contours are shown every 5 K. Their values can be ascertained by their intercepts on the lower temperature axis since there $E_k = 1.5T$. The contours for 5 and 10 K are not shown since they go through the liquid-gas coexistence region. The 15 and 20 K contours graze the corners of the liquid-gas and superfluid regions, respectively. Values inside the liquid-solid coexistence region are shown to emphasize how the contours connect across the transition. The circles are locations of the PIMC runs used to construct the fit, and the stars the locations of the new neutron scattering experiments.

(less than 1 K) on crystal structure. Throughout the density range of our present measurements, and others using identical techniques [5], there is agreement between measured and PIMC values with an average difference of 0.6 K as shown in Fig. 3(a). Figure 3(b) explicitly shows the kinetic energy changes along melting-curve isochores.

Remarkably, the contours of kinetic energy are almost continuous (to within 5%) across the melting line. In fact, the kinetic energy at constant density *increases* slightly at melting on the order of 2–4 K as shown in Fig. 3(b). The positive jump upon melting extends up to room temperature [14]. Evidently, atoms are slightly more successful in avoiding each other in the solid. The near agreement of the kinetic energy in the liquid and solid at melting comes about because the local order in the two phases is so similar. Note the comparison of the pair correlation functions in Fig. 4. Inclusion of vacancies in the solid phase lowers the jump, but it still remains positive.

On the other hand, Bafile *et al.* [8] claim a contrary *decrease* in the kinetic energy on melting, on the basis of extrapolations of liquid and solid kinetic energies across the physical density gap of their measured 4.35 K isotherm. We note that their "liquid" fit includes a substantial portion of the two-phase l-g region (see Fig. 2). As shown in Fig. 3(b), these contradictions with the present work are of sign, not just of magnitude. We believe their incorrect conclusions are based partly on measurement errors in the solid phase, and partly on inappropriate fitting functions in both phases. The solid-phase density dependence of E_k given by Bafile *et al.* [8] differs substantially from both the present results and all previous work [5,11,13,15,16], as shown in Table I. The previous results in the table apply to a variety of temperatures, but, as is evident in Fig. 2, temperature corrections are much smaller than the disagreement displayed between the Bafile *et al.* work and all others.

The liquid contours of kinetic energy are nearly horizontal at freezing indicating that, even at 40 K, helium is still a quantum liquid. We mean by this that the kinetic energy is much greater than the classical $\frac{3}{2}k_BT$ value. Such quantum behavior continues at least up to room temperature melting (Ref. [14]).

In the high temperature fluid, the *excess kinetic energy* $E_k - \frac{3}{2}k_BT$ drops off exceedingly slowly with increasing temperature as shown in Fig. 5, for low densities. In the high temperature regime, cluster expansion methods [17] are appropriate. The partition function, and hence the kinetic energy, can be expanded in powers of the fugacity,

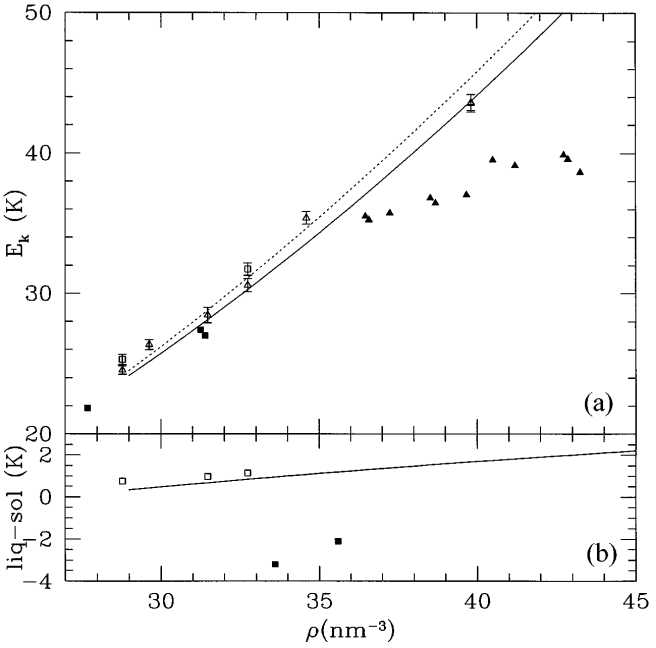

FIG. 3. (a) Density dependence of the kinetic energy of normal liquid and solid ^{4}He along the melting curve. Our measured values are shown as open squares (liquid) and triangles (solid) (Ref. [5] and present work). The fitted PIMC kinetic energy is the dotted line in the liquid and full line in the solid. Kinetic energies from Ref. [8] are shown as filled triangles (solid) and filled squares (liquid). (b) The differences between the kinetic energies of solid and normal liquid ^{4}He as a function of density. Our measured values are shown as open squares (present work and Ref. [5]). The solid line is the difference of the liquid and solid PIMC kinetic energies at melting. These are opposite in sign and different in magnitude from inferences made in Ref. [8], shown as filled squares.

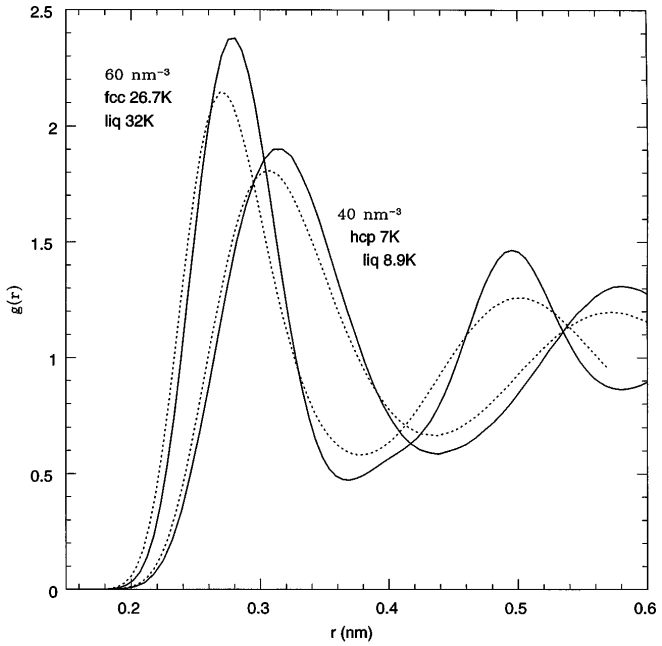

FIG. 4. Comparison of the pair correlation functions along the melting line computed with PIMC. The two left figures are at the higher density of 60 nm^{-3} and the right figures at 40 nm^{-3}. The solid lines are hcp (7 K) and fcc (26.7 K), and the dashed lines are liquid at 8.9 and 32 K.

TABLE I. Density dependences of previously published kinetic energies of hcp ^{4}He near a density of 35 atoms nm^{-3}. From Fig. 2, temperature dependence is small so these results are quoted without temperature corrections, and we assumed $E_k = 35$ K/atom.

Method	$d\ln(E_k)/d\ln(\rho)$	Reference	Year
Chopper spectrometer	1.50	[15]	1984
PIMC	1.52	[13]	1987
GFMC	1.34	[11]	1987
Chopper spectrometer	1.80	[5]	1993
SWFMC	1.76	[16]	1994
Resonance spectrometer	0.68	[8]	1995
Present fit	1.83		1996

obtaining

$$E_k \approx k_B T\left[\frac{3}{2} + \frac{\rho}{2}\int d^3r \exp[-u(r,T)]\frac{du(r,T)}{d\ln m} + \mathcal{O}[\rho^2]\right], \quad (1)$$

where $u(r,T)$ is the exact two-particle quantum action (on the diagonal) and m the atomic mass [2]. This virial correction is shown in Fig. 5. It decays roughly as $T^{-0.3}$. The near agreement at low density and high temperature shows that the slow decay of the excess kinetic energy arises from two-body scattering. By examining several similar repulsive potentials, we have observed that a steep intermolecular potential leads to a very slowly decaying excess kinetic energy. The exponent -0.3 reflects the steepness of the potential that is sampled by thermal and quantum excitations in the range $1.5 < r < 2.5$ Å.

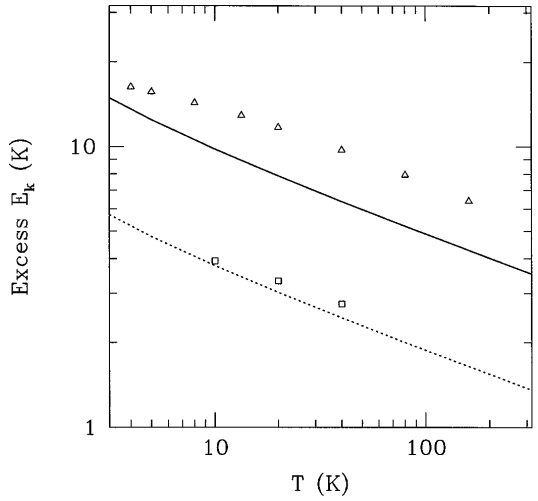

FIG. 5. The excess kinetic energy as a function of temperature at two densities: triangles (26 nm^{-3}) and squares (10 nm^{-3}). The solid and dashed lines are the excesses computed using the first-order cluster expansion, Eq. (1), at the same densities. The density matrix was calculated using the matrix squaring method [2].

In conclusion, recent experiments and calculations have, for the first time, given a global picture of the dependence of kinetic energy on density and temperature of condensed helium, the prototypical many-body quantum system.

This work was supported by the U.S. National Science Foundation under Grant No. DMR 94-224-96 and by the U.S. Department of Energy, Basic Energy Sciences-Materials Sciences under Contract No. DEFG02-91ER45439. The experimental measurements were made at the Argonne National Laboratory Intense Pulsed Neutron Source, supported by U.S. Department of Energy Contract No. W-31-109-ENG-38.

[1] R. A. Aziz, F. R. W. McCourt, and C. C. K. Wong, Mol. Phys. **61**, 1487 (1987).
[2] D. M. Ceperley, Rev. Mod. Phys. **67**, 279 (1995), and references therein.
[3] R. O. Simmons, Z. Naturforsch. **48a**, 415 (1993), and references therein.
[4] R. O. Simmons, Can. J. Phys. **65**, 1401 (1987).
[5] R. C. Blasdell, D. M. Ceperley, and R. O. Simmons (to be published).
[6] R. C. Blasdell, J. M. Carpenter, and R. O. Simmons (unpublished).
[7] V. F. Sears, Phys. Rev. B **30**, 44 (1984).
[8] U. Bafile, M. Zoppi, F. Barocchi, R. Magli, and J. Mayers, Phys. Rev. Lett. **75**, 1957 (1995).
[9] A. Driessen, E. van der Poll, and I. F. Silvera, Phys. Rev. B **33**, 3269 (1986).
[10] S. Moroni, S. Fantoni, and G. Senatore, Phys. Rev. B **52**, 13 547 (1995).
[11] P. Whitlock and R. M. Panoff, Can. J. Phys. **65**, 1409 (1987).
[12] D. M. Ceperley and E. L. Pollock, Can. J. Phys. **65**, 1416 (1987).
[13] D. M. Ceperley, in *Momentum Distributions*, edited by R. Silver and P. E. Sokol (Plenum, New York, 1987), p. 71; Z. Naturforsch. **48a**, 433 (1993).
[14] M. Boninsegni, C. Pierleoni, and D. M. Ceperley, Phys. Rev. Lett. **72**, 1854 (1994).
[15] R. O. Hilleke, P. Chaddah, R. O. Simmons, D. L. Price, and S. K. Sinha, Phys. Rev. Lett. **52**, 847 (1984).
[16] T. McFarland, S. A. Vitello, L. Reatto, G. V. Chester, and M. H. Kalos, Phys. Rev. B **50**, 13 577 (1994).
[17] B. Kahn and G. E. Uhlenbeck, Physica (Amsterdam) **5**, 399 (1938).